Vortex dynamics in regular arrays of asymmetric pinning centers

B. Y. Zhu,[1,2] L. Van Look,[1] V. V. Moshchalkov,[1] B. R. Zhao,[2] and Z. X. Zhao[2]
[1]*Laboratorium voor Vaste-Stoffysica en Magnetisme, Katholieke Universiteit Leuven, Celestijnenlaan 200D, B-3001 Leuven, Belgium*
[2]*National Laboratory for Superconductivity, Institute of Physics and Center for Condensed Matter Physics, Chinese Academy of Sciences, Beijing 100080, China*

(Received 9 May 2000; revised manuscript received 16 February 2001; published 1 June 2001)

Molecular-dynamics simulations of the current-voltage characteristics $V(I)$ have been performed for regular arrays of asymmetric pinning centers modeled by the superposition of two interpenetrating square lattices of weak and strong pinning centers with separation Δp. In this case, an applied Lorentz force $\mathbf{F}_L$ acts as a depinning force which is directed either from weak to strong pinning site or vice versa, depending on the polarity of $\mathbf{F}_L$. This leads to a pronounced asymmetry of the current-voltage characteristics and of the critical currents $I_c(\mathbf{F}_L)$ and $I_c(-\mathbf{F}_L)$ (''vortex diode effect''). In addition to that, the F_L-Δp phase diagram reveals a strong dependence of the different dynamical vortex phases on the shift between the two pinning sublattices.

DOI: 10.1103/PhysRevB.64.012504 PACS number(s): 74.60.Ge, 74.25.Dw, 74.60.Jg

The introduction of nanoengineered regular pinning arrays opens new possibilities to investigate the vortex dynamics in the mixed-state of type-II superconductors.[1–7] Commensurability effects between the flux line lattice (FLL) and the lattice of pinning sites result in a rich phase diagram demonstrating the complex behavior of the vortex motion.[8] Critical current J_c and magnetization measurements on superconductors with a triangular or square array of artificial defects (antidots or magnetic dots) have demonstrated the presence of peaks or cusps at specific magnetic field values, or ''matching fields'' $H=H_\phi$.[2–7] Very recently, experiments on superconducting thin films covering rectangular submicrometer magnetic dot arrays have revealed interesting new features of the vortex pinning.[6] The reduced symmetry of the array of pinning centers leads to a reconstruction of the vortex lattice from rectangular to square in increasing magnetic field. Further investigation of the effect of reducing the symmetry of the pinning array and the pinning sites themselves, will certainly broaden our understanding of vortex pinning and dynamical phase transitions in artificially nanostructured superconductors. A simple but effective way to model asymmetric pinning sites, is to superpose two interpenetrating arrays of weak and strong pinning centers.

In the present work, using molecular-dynamics (MD) simulations, we study the effect of asymmetry of the pinning sites on the depinning transition and on the dynamical phases of the driven vortex lattice. We focus on the incommensurate case of $H/H_\phi=1.05$, where H_ϕ is the field at which the number of vortices N_v is equal to the number of strong (or weak) pinning sites $N_p^s(N_p^w)$. We have found that, for the two interpenetrating pinning arrays with separation Δp, the direction of the applied Lorentz force plays an important role in the FLL depinning and motion, which results in an asymmetric current-voltage characteristic. We will also show that for $H/H_\phi=1.05$, the critical Lorentz force needed for the FLL depinning as well as the dynamical vortex phases depend on the shift between the two pinning sublattices.

The geometry of the two-dimensional (2D) interpenetrating arrays of weak and strong pinning centers is shown schematically in Fig. 1. Both the strong and the weak pinning sites form perfect square lattices. The spacing a_0 between the pinning sites of the strong and the weak pinning array is the same, which we define as $a_0=1$.

We model all pinning centers by Gaussian potential wells with a decay length R_p.[9–11] The pinning force is taken as

$$\mathbf{F}_p(\mathbf{r}_i)=\sum_{\Gamma=w,s}\left[-F_{p0}^{\Gamma} f_0 \sum_k^{N_p^{\Gamma}} \frac{\mathbf{r}_i-\mathbf{R}_k^{\Gamma}}{R_p}\exp\left(-\left|\frac{\mathbf{r}_i-\mathbf{R}_k^{\Gamma}}{R_p}\right|^2\right)\right], \tag{1}$$

where $\mathbf{r}_i$ represents the location of the ith vortex and $\Gamma=w$(''weak'') or s(''strong''). $\mathbf{R}_k^w$ ($\mathbf{R}_k^s$) stands for the location of the kth weak (strong) pinning site in the 2D system. $F_{p0}^w f_0$ ($F_{p0}^s f_0$) denotes the intensity of the weak (strong) individual pinning force. In our simulations all forces are taken in units of $f_0=\Phi_0^2/8\pi^2\lambda^3$, with Φ_0 the superconducting flux quantum and λ the superconducting penetration depth. The shift between the two pinning sublattices Δp determines the shape of asymmetric periodic potential as can be seen in Fig. 2, where we show the periodic asymmetric pinning potentials along the y direction for various Δp. The applied driving force acting on the vortices is the Lorentz force $\mathbf{F}_L=\mathbf{J}\times\mathbf{\Phi}_0$, where $\mathbf{J}$ is the applied current. In the

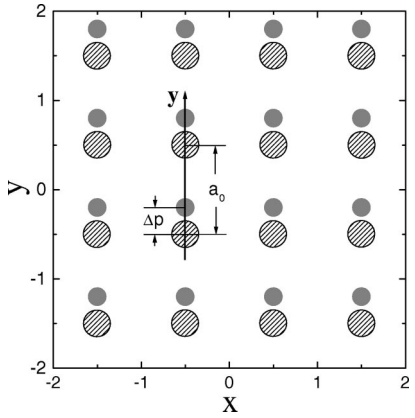

FIG. 1. An illustration of the two interpenetrating square lattices of pinning centers. The period of both the strong pinning lattice (big hatched circles) and the weak pinning lattice (small grey circles) is the same. Δp denotes the shift between the strong and the weak pinning lattice along the y direction.

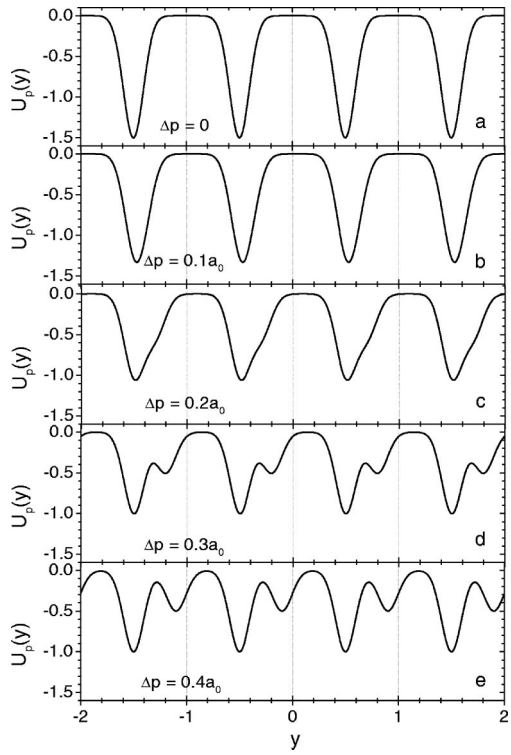

FIG. 2. The pinning potentials created by the two sets of square pinning sites (strong $F_{p0}^{s}=1$ and weak $F_{p0}^{w}=0.5$) for different shifts $\Delta p=a_0 \times 0.0$, 0.1, 0.2, 0.3, and 0.4 in (a)–(e), respectively.

present simulation, the external current is applied along the x direction in the x-y plane, so the driving Lorentz force $\mathbf{F}_L$ is always parallel to the y axis, i.e., $F_L \equiv F_{Ly}$. The repulsive intervortex interaction is modeled using the modified Bessel function K_1 (Refs. 10,11) and the intervortex interacting force is given by

$$\mathbf{F}_{vv}(\mathbf{r}_i)=F_{vv0}\,f_0\sum_{j\neq i}^{N_v} K_1\left(\frac{\mathbf{r}_i-\mathbf{r}_j}{\lambda}\right)\mathbf{r}_{ij}, \tag{2}$$

where $\mathbf{r}_{ij}=(\mathbf{r}_i-\mathbf{r}_j)/|\mathbf{r}_i-\mathbf{r}_j|$. $F_{vv0}\,f_0$ denotes the intensity of the intervortex interacting force and the cutoff length for this long-range force is taken as 4λ. As a result, the overdamped equation of the vortex motion without thermal fluctuations is given by

$$\eta\mathbf{v}_i=\mathbf{F}_L+\mathbf{F}_{vv}(\mathbf{r}_i)+\mathbf{F}_p(\mathbf{r}_i), \tag{3}$$

where η is the viscosity coefficient and taken to be unity.

In our simulation, the equation is solved by taking discrete time steps Δt in a 2D square sample with side $20a_0=20$ containing two interpenetrating strong and weak pinning arrays ($N_p^w=N_p^s=400$) with periodic boundary conditions in both directions. The other fixed lengths and forces used in the simulations are $R_p=0.13$, $\lambda=3.6$. $F_{vv0}=0.1$, $F_{p0}^{w}=0.5$, and $F_{p0}^{s}=1$. We have also employed the same numerical simulations on a sample of various sizes but with the same vortex density and pinning configuration. The presented results are insensitive to the sample size, provided the density of vortices and pinning sites remains unchanged.

To investigate the effect of the asymmetric pinning potential on the vortex motion, it is interesting to vary the displacement of the two pinning sublattices and to change the polarity of the applied driving force in the y direction. This can be achieved either by fixing the applied driving force polarity along the y direction and changing the shift between the strong and the weak pinning sublattices from $-a_0/2$ to $a_0/2$ (see Fig. 1), or by varying the shift between the strong and weak pinning sites from 0 to $a_0/2$ and alternating the polarity of the applied driving force. Both methods yield the same result. In the present simulation, we always take the latter to calculate the dependence of the depinning Lorentz force on the asymmetry of the pinning sites.

We have studied the influence of the asymmetric pinning potential on the dynamical vortex phase transitions for the incommensurate case $H/H_\phi=1.05$. We obtain the initial vortex configuration by an annealing course in the case of $\Delta p=0$. After this procedure, all strong (or weak) pinning are occupied by one vortex, and the remaining 5% of H_ϕ vortices are located at interstitial positions. In our calculation, each pair of current-voltage curves $v_y(F_L)$ is obtained by increasing the driving force F_L from zero with a small step $\Delta F_L=0.0005$ starting from the same initial vortex configuration. At each F_L value, we always neglect the first 100 MD steps and average the following 400 ones. The final vortex configuration obtained for F_L is used as the starting configuration for the calculation at $F_L+\Delta F_L$. Figure 3 shows the average velocity of all vortices v_y as a function of the driving Lorentz force F_L for different shifts Δp between the strong and weak pinning sublattices. The velocity versus driving force plots correspond to the experimental voltage-current $V(I)$ curves. We observe several remarkable features due to the presence of the asymmetric pinning potential.

In order to characterize the evolution of the dynamical vortex phases with respect to the shift Δp between the pinning sublattices, we show first the current voltage curves for $\Delta p=0$ in Fig. 3(a). In this case, the two pinning sublattices overlap, resulting in $v_y(F_L)$ curves which are symmetric with respect to the sign of F_L. The observed dynamical phases are exactly the ones expected for a symmetric square pinning potential, and are very similar to the results reported by Reichhardt *et al.*[8] At low drive the vortices remain pinned, forming a flux solid, phase I. As the driving Lorentz force is increased beyond a critical value F_L^c, the interstitial vortices depin resulting in a 1D interstitial flow (phase II). The phases for higher F_L values are disordered 2D flow (phase III), incommensurate 1D flow (phase IV), and the incommensurate and commensurate flow (phase V), respectively.

As seen in Fig. 3(b), a small shift Δp between the pinning sublattices results in almost identical transitions from the pinned phase I to phase II, where the interstitial vortices are depinned, for both positive and negative signs of $\mathbf{F}_L$. However, a weak asymmetry of the other phase transitions is observed. Moreover, the feature typical for the phase III, i.e., a noisy $v_y(F_L)$ curve associated with the disordered 2D vortex flow, becomes weak in this case. It is interesting to note that for this small shift of the two interpenetrating pinning arrays ($\Delta p=0$ or $0.1a_0$), the strong and the weak pinning potentials overlap to a large extent, and the resulting pinning potential well becomes quite deep [see Fig. 2(a),2(b)]. This is why the positive and the negative Lorentz forces leading

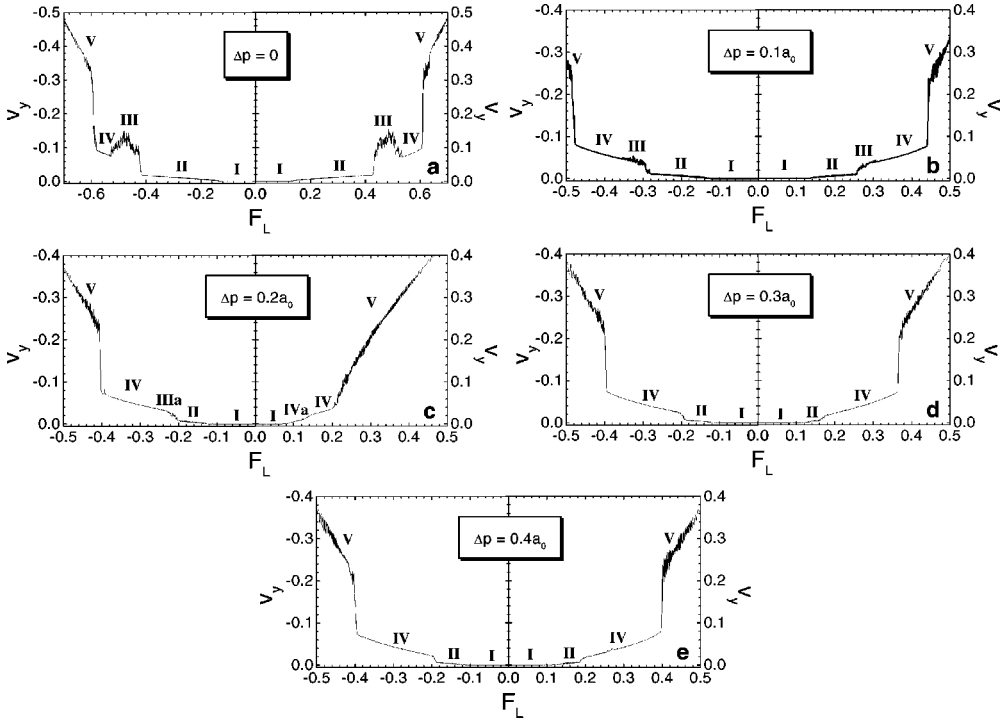

FIG. 3. The dependence of the average velocity v_y on the external Lorentz force F_L for different shifts between the two sets of interpenetrating square pinning arrays. $\Delta p = a_0 \times 0.0$, 0.1, 0.2, 0.3, and 0.4 for (a)–(e), respectively. The simulations are carried out for the magnetic field slightly higher than the first matching field, i.e., $H/H_\phi = 1.05$.

to depinning of all vortices in the system, i.e., at the transition from phase IV to phase V, are large in this case. With the increase of the shift Δp, the asymmetry between the positive and the negative phase boundaries becomes more pronounced, as shown in Figs. 3(c)–3(e). We find that in the case of the Lorentz driving force applied along the negative y direction, i.e., pointing from the weak pinning site towards the strong one, the critical driving force F_L^c for the IV-V phase transition decreases, while the critical driving force for the I-II phase transition is not sensitive to the increase of Δp. For the Lorentz driving force along the positive y direction, i.e., pointing from the strong pinning site towards the weak one, the threshold value of F_L for each phase boundary drops rapidly to a minimum at $\Delta p \simeq 0.2a_0$ and then gradually recovers up to the saturation at large Δp. In addition to that, in the case of $\Delta p \simeq 0.2a_0$, we observe clearly that the phase III (disorder 2D vortex flow) completely disappears. Instead, we find the phases IVa, characterized by 1D zigzag flow in the positive y direction of $\mathbf{F}_L$, and IIIa, where 2D partially disordered flow occurs, when $\mathbf{F}_L$ is along the negative y direction. Another phase, named IIIb which shows 2D ''spindle'' flow, also appears for $\Delta p = 0.12a_0$. These vortex flow patterns, which we contribute to the effect of the asymmetric pinning arrays, cannot be found in the symmetric periodic pinning system. The vortex trajectories of these new dynamical phases IVa, IIIa, and IVb are shown in Figs. 4(a)–4(c), respectively.

In Fig. 3(d), one can find that besides some asymmetric structures between the $v_y(F_L)$ curves for positive and negative F_L orientations, the phase between II and IV disappears completely, because of the weak pinning effects when the two sets of pinning centers are separated. This result is similar to the case of a symmetric periodic pinning array of weak pinning centers.[8]

The Lorentz forces F_L, for which the transitions between the different dynamical vortex phases occur, are shown as a function of the shift Δp between the two pinning lattices in the F_L-Δp phase diagram (Fig. 5). For $\Delta p = 0$, all phases (I to V) are symmetric. With increasing Δp, the asymmetry between the two Lorentz force directions appears, both in the critical depinning force F_L^c (open squares in Fig. 5) and in the onset of the different dynamical phases II to V (circles, up and down triangles in Fig. 5). The highest asymmetry can be found for $\Delta p = 0.2a_0$. For large separation between the two pinning sublattices ($0.4a_0 < \Delta p < 0.5a_0$), a symmetrical behavior with respect to the Lorentz force direction is seen again. To analyze the asymmetry of the critical driving force F_L^c and the dynamical phase transitions, we consider the evolution of the pinning potential well as a function of the shift

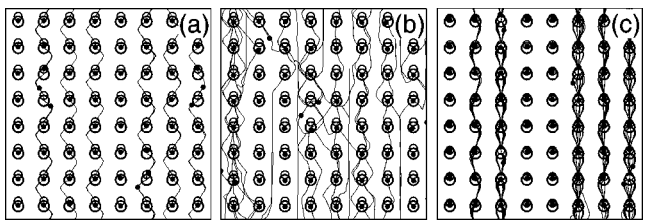

FIG. 4. Trajectories of the new dynamical vortex phases caused by asymmetric pinning centers. (a) IVa, 1D zigzag flow; (b) IIIa, 2D partially disordered flow; (c) IVb, 2D ''spindle'' flow. The vortices are represented by black dots and the strong and weak pinning sites by big and small open circles, respectively.

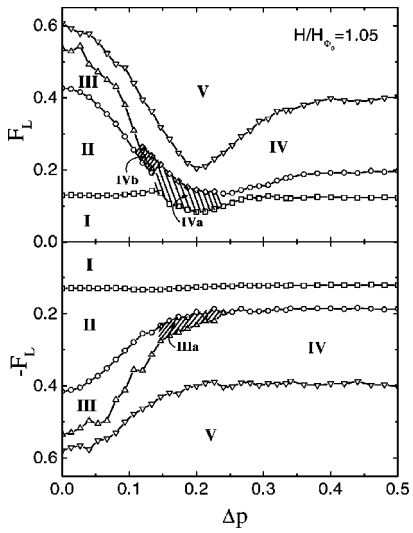

FIG. 5. Dynamical phase diagrams for the FLL motion as a function of the shift between the strong and the weak pinning lattice Δp. Here, $H/H_\phi = 1.05$, $F_{p0}^s = 1$, $F_{p0}^w = 0.5$. The same initial FLL configuration is used for the simulation in the two directions.

between the sublattices Δp (Fig. 2). For small shifts, the presence of the sublattice of weak pinning centers is hardly visible and it results only in the asymmetry of the slopes of the potential wells $U_p(y)$ [see Figs. 2(a),2(b)]. Since the derivative $-dU_p/dy$ defines the pinning force, the asymmetry of the slopes will be reflected in the asymmetry of the critical Lorentz force (open squares in Fig. 5). It is clear that in this case it is easier to depin the vortex lattice by applying a current which creates a driving Lorentz force in the positive y direction (see Fig. 1). By increasing the shift between the two pinning sublattices, separate weak pinning sites are formed which are still partially overlapping with the strong pinning centers nearby [see Fig. 2(d)]. These weak pinning sites assist the onset of the vortex motion only in one direction: from strong to weak pinning site. Therefore, the critical depinning force F_L^c (open squares in Fig. 5) is lowered significantly at $\Delta p = 0.2a_0$ for positive $\mathbf{F}_L$. Additionally, the transition between the dynamical vortex phases II to V also occurs at a lower F_L. The assisting role of weak pinning sites, however, is completely lost when the two interpenetrating sublattices are well separated [Fig. 2(e)] and thus the symmetry of the depinning Lorentz force is fully recovered [see Figs. 3(e) and 5].

The superconductor with an array of pinning sites, asymmetric along the y direction, appears to function as a ''vortex diode'' impeding flow in one direction but not in the other,[12] due to the difference in the critical driving forces. As seen in Fig. 5, the ''vortex diode'' or ''one-way valve'' for vortex motion can be adjusted by varying the shift of the two sets of pinning sublattices. A similar result has been found recently for the ''ratchet effect''[13] for the removal of the vortices out of a superconducting sample.

To demonstrate that the ''vortex diode'' effects are not restricted to the case $H/H_\phi > 1$, we have examined the case $H/H_\Phi < 1$. Also here, the asymmetry of the critical depinning force and the dynamical vortex phases with respect to the direction of the Lorentz force have been revealed.

In conclusion, we have observed a pronounced asymmetry in the critical depinning forces and in the behavior of the dynamical vortex phases in regular pinning arrays consisting of two interpenetrating square lattices of weak and strong pinning centers. We have demonstrated that these asymmetric pinning sites can act as ''vortex diodes,'' allowing vortex flow only in one direction. The shift between the two pinning sublattices Δp can significantly change the asymmetry of the vortex mobility, as was summarized in the F_L-Δp phase diagram. Novel dynamical vortex phases, characteristic for asymmetric pinning arrays, have been found.

This work was supported by the ESF Program VORTEX, the bilateral BIL 97/35 China/Flanders Project and Belgian IUAP, the Flemish GOA and FWO Programs, and the National Natural Science Foundation of China.

[1] K. Harada, O. Kamimura, H. Kasai, T. Matsuda, A. Tonomura, and V. V. Moshchalkov, Science **274**, 1167 (1996), and references therein.

[2] J. I. Martín, M. Vélez, J. Nogues, and I. K. Schuller, Phys. Rev. Lett. **79**, 1929 (1997).

[3] V. V. Moshchalkov, M. Baert, V. V. Metlushko, E. Rosseel, M. J. Van Bael, K. Temst, Y. Bruynseraede, and R. Jonckheere, Phys. Rev. B **57**, 3615 (1998).

[4] V. V. Moshchalkov, M. Baert, V. V. Metlushko, E. Rosseel, M. J. Van Bael, K. Temst, R. Jonckheere, and Y. Bruynseraede, Phys. Rev. B **54**, 7385 (1996).

[5] M. Baert, V. V. Metlushko, R. Jonckheere, V. V. Moshchalkov, and Y. Bruynseraede, Phys. Rev. Lett. **74**, 3269 (1995).

[6] J. I. Martín, M. Vélez, A. Hoffmann, I. K. Schuller, and J. L. Vicent, Phys. Rev. Lett. **83**, 1022 (1999).

[7] M. J. Van Bael, K. Temst, V. V. Moshchalkov, and Y. Bruynseraede, Phys. Rev. B **59**, 14 674 (1999); M. J. Van Bael, J. Bekaert, K. Temst, L. Van Look, V. V. Moshchalkov, Y. Bruynseraede, G. D. Howells, A. N. Grigorenko, S. J. Bending, and G. Borghs, *ibid.* **86**, 155 (2001).

[8] C. Reichhardt, C. J. Olson, and F. Nori, Phys. Rev. Lett. **78**, 2648 (1997); Phys. Rev. B **58**, 6534 (1998). These papers describe the dynamical vortex phases and also show the corresponding vortex trajectories.

[9] K. Moon, R. T. Scalettar, and G. T. Zimanyi, Phys. Rev. Lett. **77**, 2778 (1996).

[10] A. Brass and H. J. Jensen, Phys. Rev. B **39**, 9587 (1989); H. J. Jensen, A. Brass, A. C. Shi, and A. J. Berlinsky, *ibid.* **41**, 6394 (1990).

[11] B. Y. Zhu, D. Y. Xing, J. Dong, and B. R. Zhao, Physica C **311**, 140 (1999); B. Y. Zhu, J. Dong, and D. Y. Xing, Phys. Rev. B **57**, 5063 (1998).

[12] F. Pardo, F. De La Cruz, P. L. Gammel, E. Bucher, C. Ogelsby, and D. J. Bishop, Phys. Rev. Lett. **79**, 1369 (1997).

[13] C. S. Lee, B. Janko, I. Derenyi, and A.-L. Barabasi, Nature (London) **400**, 337 (1999).